# Tunable Dispersion Compensator Using PLC Type Optical Transversal Filter

*by Hiroshi Kawashima *, Noritaka Matsubara * and Kazutaka Nara **

**ABSTRACT** In high bit rate optical transmission systems such as 40 Gbps, dispersion tolerances will be smaller than the dispersion fluctuations due to such factors as temperature change or power variation. To compensate for these fluctuations, tunable dispersion compensators (TDCs) are needed. Various types of tunable dispersion compensators have been demonstrated. Of these, integrated optic finite impulse response filter type TDCs in silica-based planar lightwave circuits (PLCs) are promising because of their flexibility with respect to dispersion curve shape, tunability of center wavelength and ability to compensate for multiple channels. Among these, the transversal filter, consisting of a splitter, N delay lines (called taps) connected in parallel and a combiner, is capable of having a large number of taps for high resolution and high controllability using monitor waveguides.
Owing to these advantages, we have fabricated an 8-tap transversal filter type TDC in a silica-based PLC with a high index contrast of 1.5 %, and have confirmed its operating principle using two types of dispersion curve shapes. We have been able to obtain good performance: chromatic dispersion of −71 ～ +109 ps/nm, insertion loss of <10 dB and operating wavelength range of 0.5 nm. We have also fabricated a 16-tap transversal filter type TDC and have confirmed a higher resolution than the 8-tap TDC.

## 1. INTRODUCTION

High bit rate optical transmission systems such as 40-Gbps systems are about to be introduced in backbone networks to meet rapid traffic increases in broadband access networks with FTTH or xDSL.

In such high bit rate systems, dispersion tolerances will be smaller than the dispersion fluctuations due to such factors as temperature change or power variation, and this will cause deterioration in transmission quality. To compensate for these fluctuations, adaptive tunable dispersion compensators (TDCs) are needed. Various types of TDCs based on FBGs, bulk optics and integrated optics have been demonstrated [1)~3)]. Of these, integrated optic finite impulse response (FIR) filter type TDCs such as lattice filters and transversal filters in silica-based planar lightwave circuits (PLCs) are promising because of their flexibility with respect to dispersion curve shape, tunability of center wavelength and ability to compensate for multiple channels [3)]. The FIR filters have N delay lines (called taps) configured with multiple Mach-Zehnder interferometers (MZIs), and the desired filter characteristics can be obtained according to arbitrary tap coefficients that determine the amplitude and phase of optical signals in each tap. Among these, the transversal filter, which consists of a splitter, N taps connected in parallel and a combiner, has a number of advantages such as the possibility of having a large number of taps for high resolution and high controllability of tap coefficients by use of pre-existing idle ports of MZIs in the splitters and combiners as monitor waveguides without additional losses [4)].

Owing to these advantages, we have designed a transversal filter type TDC for 40-Gbps systems using discrete Fourier transformation, have fabricated an 8-tap transversal filter type TDC in a silica based PLC with a high index contrast of 1.5 %, and have confirmed the operating principle using two types of dispersion curve shapes. We have thus been able to obtain good performance: chromatic dispersion of −71 ～ +109 ps/nm, insertion loss of <10 dB and operating wavelength range of 0.5 nm [6)]. In addition, we have fabricated a 16-tap transversal filter type TDC and have confirmed a higher resolution than the 8-tap TDC.

## 2. CIRCUIT CONFIGURATION

Figure 1 shows the configuration of the 8-tap transversal filter type TDC that we have fabricated. The filter has three sections: a variable splitter, delay lines with variable phase shifters (VPSs) and a variable combiner. The variable splitter and the variable combiner consist of the same three-stage cascaded variable couplers (VCs) using MZIs, and are designed symmetrically having mirror image characteristics so that the filter has a low theoretical loss. In this

* FITEL-Photonics Lab., R&D Div.

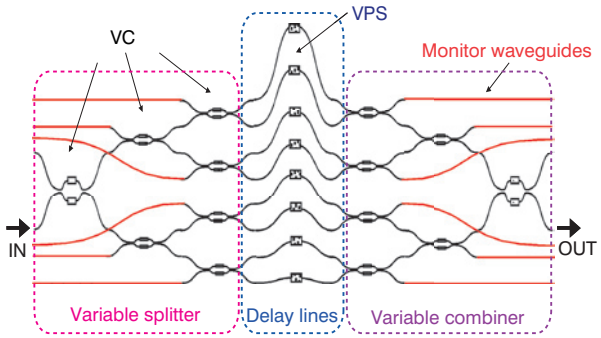


**Figure 1 Schematic configuration of transversal filter type TDC.**

circuit configuration, we can easily increase the resolution by adding VC stages and increasing the number of taps. The circuit has monitor waveguides for adjusting the circuit characteristic, which connects pre-existing idle ports of the cascaded VCs to the end of the PLC chip.

## 3. FILTER SYNTHESIS

The transfer function G of the filter is expressed by a Fourier series as,

$$G = \sum_{n=0}^{N-1} g_n \exp\left(-j\frac{2\pi}{c} n_{\text{eff}} f n \Delta L\right) \quad (1)$$

where $n_{\text{eff}}$ is the effective refractive index of the waveguides, $f$ is the optical frequency, $n\Delta L$ is a fixed delay to each tap ($n$= 0,1...$N$−1), $c$ is the velocity of light, and $j$ is the imaginary unit; $g_{\text{n}}$ is the tap coefficient of the filter given by

$$g_n = \gamma_n \exp(j\theta_n) \quad (2)$$

where $\gamma_{\text{n}}$ is the coupling ratio of the variable splitter and variable combiner, and $\theta_{\text{n}}$ is additional phase to each tap. Discrete Fourier transformation of equation (1) gives $g_{\text{n}}$ as

$$g_n = \frac{1}{N'} \sum_{l=0}^{N'-1} G_l \exp\left(j\frac{2\pi}{N'} nl\right) \quad (3)$$

where $G_l$ is a target frequency response, and $N$' is the number of sampling data.

In this study, we used two types of target frequency response in order to ensure the flexibility of the dispersion curve shape of the filter. The first target $G_{l1}$, determined by equation (4), has a quadratic phase spectrum that results in a constant chromatic dispersion value in each free spectral range (FSR) of the filter. The second target $G_{l2}$, determined by equation (5), has a sinusoidal phase spectrum that results in a pseudo-constant chromatic dispersion value around the center of each FSR and a continuous connection with adjacent order spectra.

$$G_{l1} = \exp\left\{j\varepsilon\pi\left(\frac{2}{FSR}\right)^2(\lambda-\lambda_c)^2\right\} \quad (4)$$

$$G_{l2} = \exp\left\{j\varepsilon\pi \sin\left(2\pi\frac{\lambda-\lambda_c}{FSR}\right)\right\} \quad (5)$$

where $\lambda$ is wavelength, $\lambda_{\text{c}}$ is centre wavelength, and $\varepsilon$ is a coefficient determining the inclination of the dispersion characteristics.

Based on the above discussion, we calculated filter characteristics using $G_{l1}$ and $G_{l2}$.

Figure 2 and Figure 3 show examples of target spectra and calculated tap coefficients. The circuit parameters are shown in Table 1.

In the case of $G_{l1}$, the calculated tap coefficients are multiplied by a window function called the "Hamming window" [5] in order to reduce group delay ripples in the pass band, caused by the use of an insufficient number of taps to exactly express the target phase spectrum with sharp edges as Fourier series.

Figure 4 shows calculated group delay responses and power transmittances of the filter using $G_{l1}$ ($\varepsilon$= −2.0 ~ +2.0 ) and $G_{l2}$ ($\varepsilon$= −0.7~ +0.7). As shown in Figure 4, group delay shapes were varied as $\varepsilon$ values in both target types. As a result, a chromatic dispersion (CD) of ±93 ps/nm, a 3-dB bandwidth of about 0.3 nm and an operat-

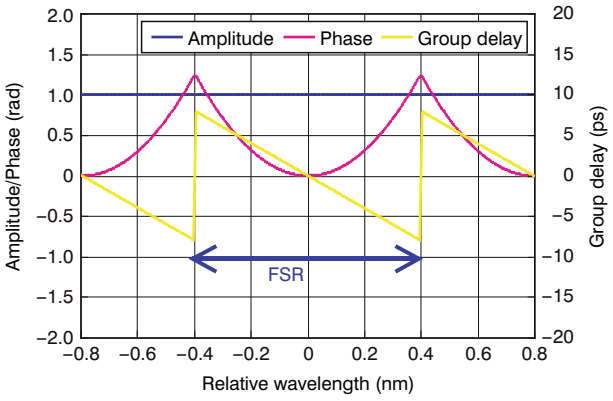


**(a) Using $G_{l1}$**

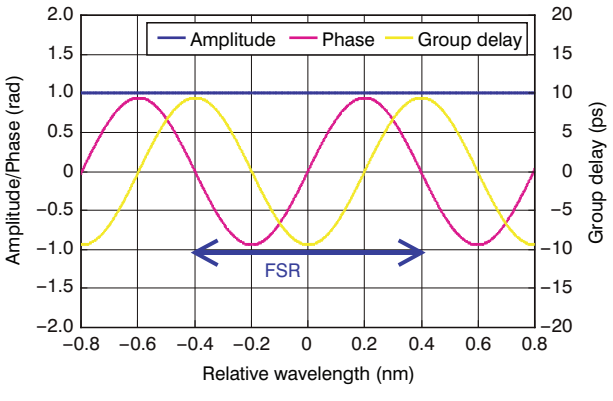


**(b) Using $G_{l2}$**

**Figure 2 Target spectra.**

**Table 1 Circuit parameters.**

| Target phase shape | Quadratic (Gl1) | Sinusoidal(Gl2) |
|---|---|---|
| Tap number | 8 | 8 |
| $\Delta L$ | 2055 $\mu$m | 2055 $\mu$m |
| FSR | 100GHz | 100GHz |
| $\lambda_C$ | 1545nm | 1545nm |
| $\varepsilon$ | −2 ~ +2 | −0.7 ~ +0.7 |

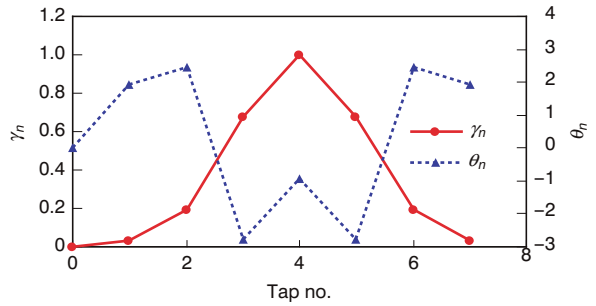


(a) Using $G_{l1}$ (FSR=100 GHz, 8 taps, $G_{l1}$, $\varepsilon$=−1)

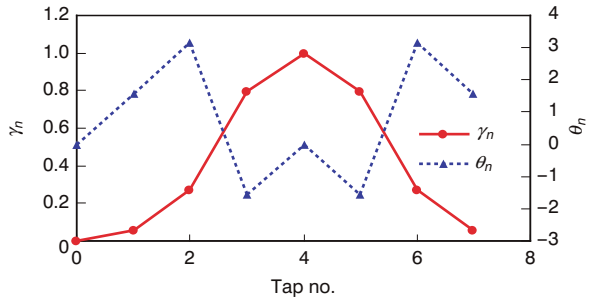


(b) Using $G_{l2}$ (FSR=100 GHz, 8 taps, $G_{l2}$, $\varepsilon$=−4)

**Figure 3 Calculated tap coefficients.**

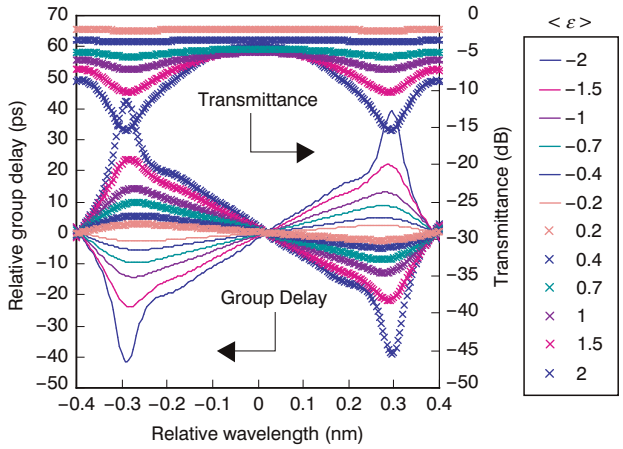


(a) Using $G_{l1}$ target (FSR=100 GHz, 8 taps)

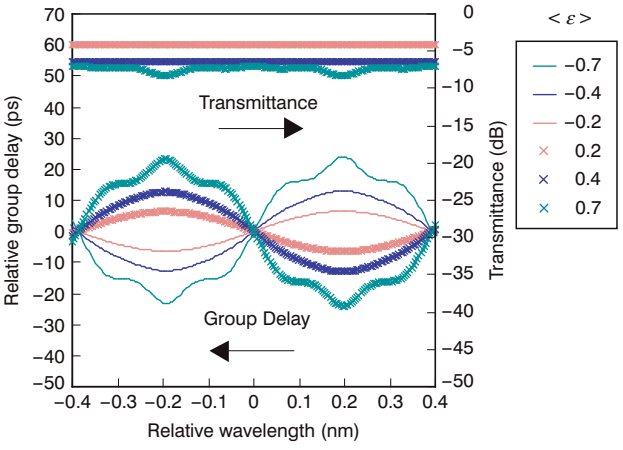


(b) Using $G_{l2}$ target (FSR=100 GHz, 8 taps)

**Figure 4 Calculated spectra.**

ing wavelength range of 0.5 nm were obtained at $\varepsilon$= ±2.0 using $G_{l1}$ and CD of ±200 ps/nm, 3-dB bandwidth of about 0.4 nm and operating wavelength range of 0.35 nm were obtained at $\varepsilon$= ±0.7 using $G_{l2}$ around the centre wavelength.

The narrower 3-dB bandwidths than the operating wavelength ranges at large $\varepsilon$ values using $G_{l2}$ are due to the window function and that limits the usable wavelength range.

We then calculated the spectra using tap numbers of 8, 16 and 32, and FSRs of 25, 50, 100 and 200 GHz. Figure 5 shows calculated maximum CD and 3-dB bandwidth vs. FSR. In the case of 32 taps in $G_{l1}$ and the case of $G_{l2}$, 3-dB bandwidths are fixed to be equal to FSR and FSR/2, respectively, because these spectra are over −3 dB in all operating wavelength ranges. As shown in Figure 5, there is a trade-off between CD and bandwidth: that is, CD is inversely proportional to FSR² whereas bandwidth is proportional to FSR. In addition, the 3-dB bandwidth becomes wider with an increase in the number of taps in

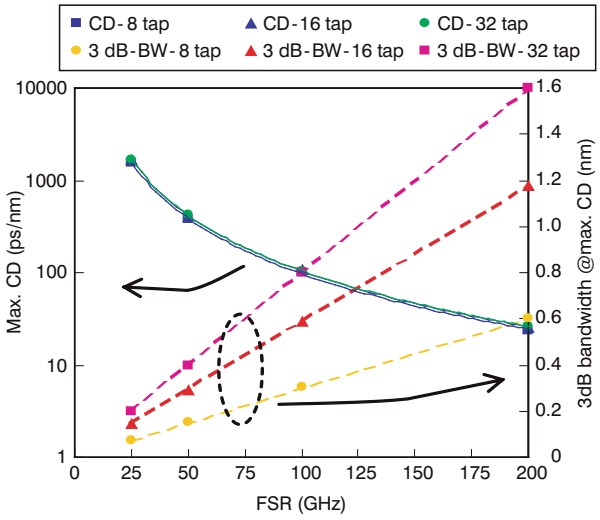


(a) Using $G_{l1}$ ($\varepsilon$=−2)

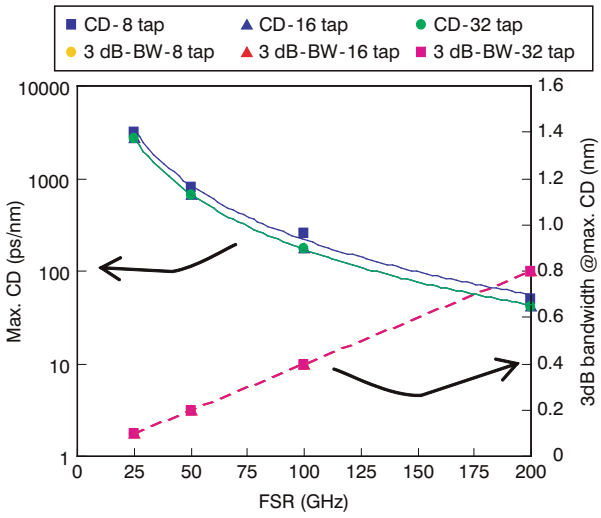


(b) Using $G_{l2}$ ($\varepsilon$=−7)

**Figure 5 Calculated maximum CD and 3-dB bandwidth vs. FSR.**

the case of $G_{l1}$, although CD shows little change with the number of taps.

From these results, we found that the suitable values for 40-Gbps systems, in which a bandwidth of 0.6 nm and a CD range of ±100 ps/nm are required, were an FSR of 100 GHz and a tap number of 16 or larger in $G_{l1}$, and an FSR of 150 GHz in $G_{l2}$.

However, a large number of taps means needing to control a large number of variable couplers and variable phase shifters, and this makes control more complicated. We therefore used an 8-tap transversal filter for the first prototype to confirm the operating principle, and after that, we tried fabricating a 16-tap transversal filter to realize higher filter resolution.

## 4. FABRICATION

Based on the above design, we fabricated a transversal filter type TDC. In order to reduce chip size, we adopted a $GeO_2$-doped silica based PLC with a high index contrast of $\Delta$=1.5 %, a minimum bending radius of 2 mm and a core size of 5 x 5 $\mu m^2$ using flame hydrolysis deposition and reactive ion etching. On the MZI arms of the variable couplers and delay lines, thin film heaters were deposited as thermo-optic phase shifters. Around the phase shifters, heat-insulating grooves were formed so that we could reduce power consumption.

Figure 6 shows the insertion loss of the high index contrast waveguide. We found that the propagation loss of the waveguide was about 0.06 dB/cm and this value is fully applicable to a large-scale circuit like this TDC. Figure 7 shows the 16-tap TDC chip that we fabricated. Because of the small bending radius of the high index contrast waveguide, we were able to use the folding arrangement illustrated in Figure 7 and realized a small chip size of 68.0 x 24.0 $mm^2$.

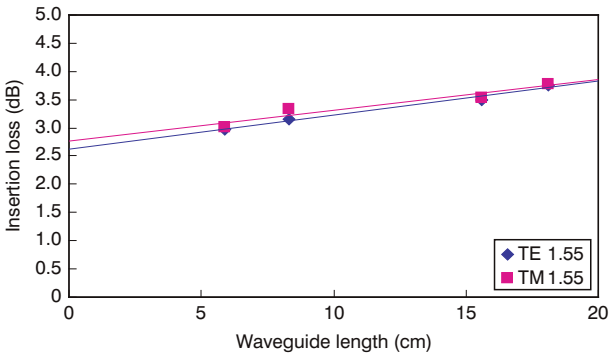


**Figure 6 Insertion loss versus waveguide length of 1.5% PLC.**

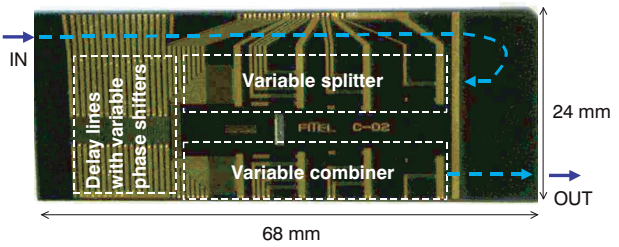


**Figure 7 16-tap transversal filter type TDC chip.**

## 5. SETTING PROCEDURE OF TAP COEFFICIENTS

In order to realize the calculated filter response exactly, we needed to set the tap coefficients precisely. However, each VC and VPS has fabrication errors. We therefore controlled the TDC by the following procedure. First we measured each variable characteristic of the VCs using monitor waveguides, and then measured the characteristics of VPSs by measuring interference spectra between adjacent VPSs. After that, we calculated phase errors caused by fabrication errors from the measured wavelength shift, and compensated for them by driving VPSs with adequate power. Finally, we set VCs and VPSs to the calculated tap coefficients using characteristics actually measured [5].

Figure 8 shows filter spectra of the 8-tap transversal filter fabricated here before and after phase error correction of the VPSs. Gray plots in each graph indicate calculated spectra. In the corrected spectra, we found that the transmittance and peak position corresponded well to the calculated spectra, showing that error correction was successfully performed.

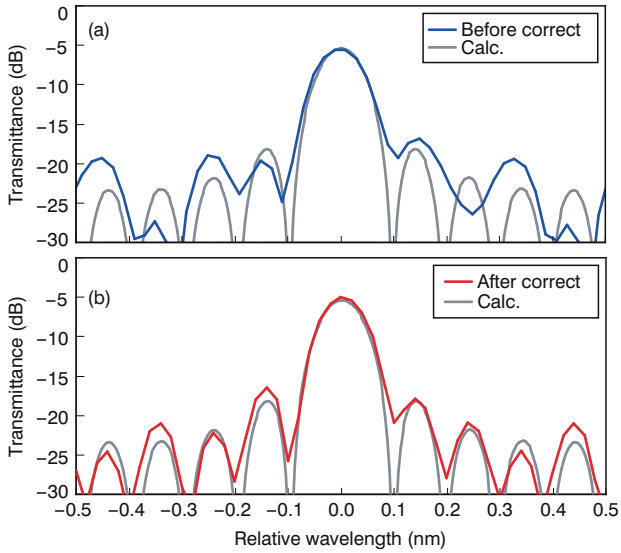


**Figure 8 Error correction result of phase shifters.**

## 6. RESULT OF MEASUREMENTS FOR 8-TAP TDC

Next, we set the tap coefficient to the values calculated for the TDC, and measured group delay and transmittance using the phase shift method. All the measurements were done using a TE polarization light around 1545 nm. During measurement the chip temperature was kept at 60 °C using a Peltier cooler in order to fix the center wavelength.

Figure 9 shows the measured spectra using $G_{l1}$ and $G_{l2}$. Gray plots in each graph indicate calculated spectra. As shown in Figure 9, the group delay shapes were success-

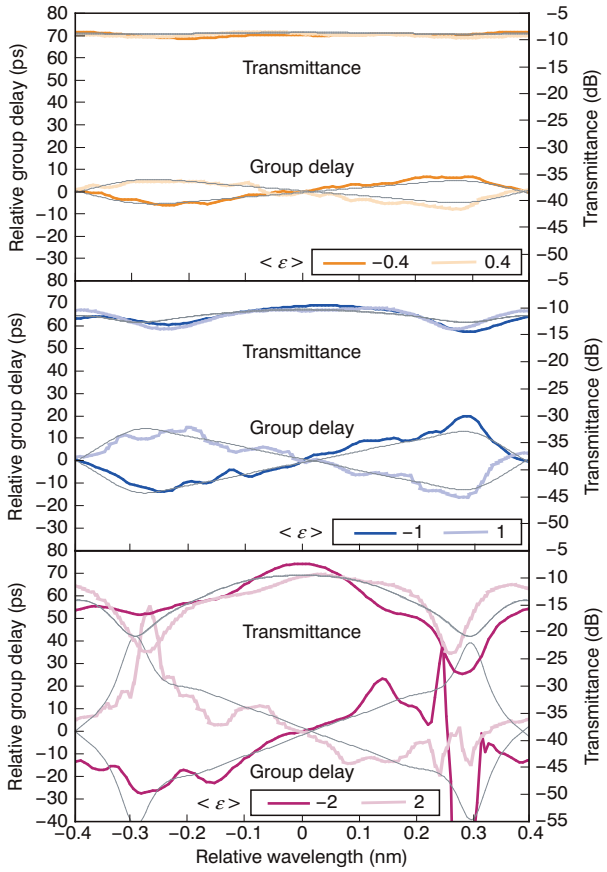


**(a) Using $G_{l1}$ target ($\varepsilon$=±0.4, 1.0, 2.0)**

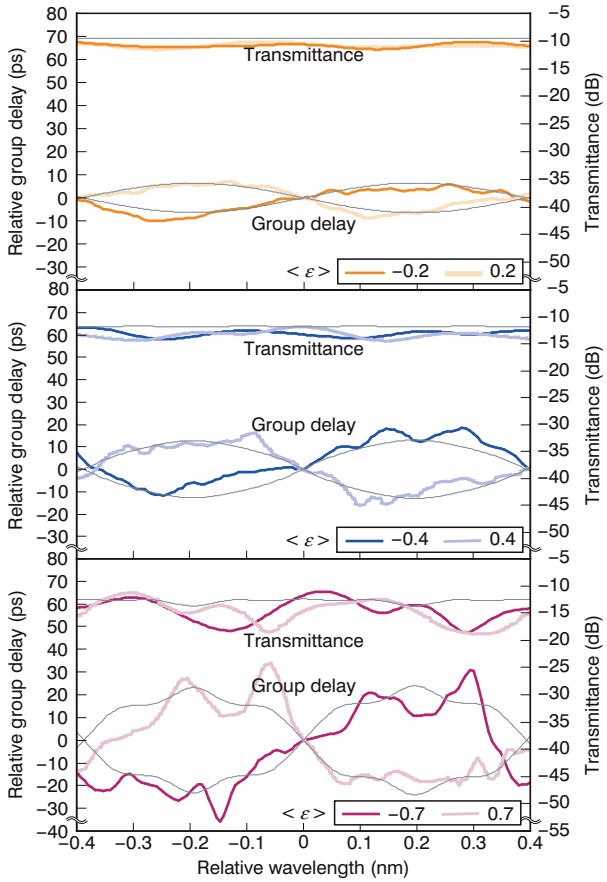


**(b) Using $G_{l2}$ target ($\varepsilon$=±0.2, 0.4, 0.7)**

**Figure 9 Measured spectra.**

fully varied as $\varepsilon$ value and mostly corresponding to the calculated ones.

Figure 10 shows CD vs. $\varepsilon$, with open plots indicating calculated values. As can be seen, CD values of −71∼−109 ps/nm with $G_{l1}$ and −203∼+121 ps/nm with $G_{l2}$ were observed, and showed good agreement with the calculated values. The measured values for insertion loss, 3-dB bandwidth and operating wavelength range were about 10 dB, 0.2 nm and 0.5 nm for $G_{l1}$ and 13 dB, 0.2 nm and 0.35 nm for $G_{l2}$.

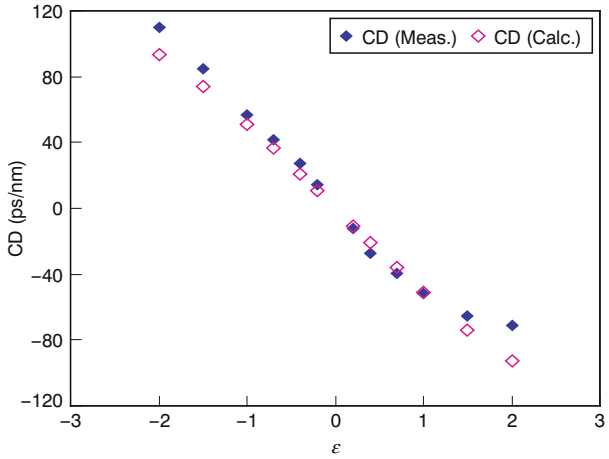


**(a) Using $G_{l1}$ target**

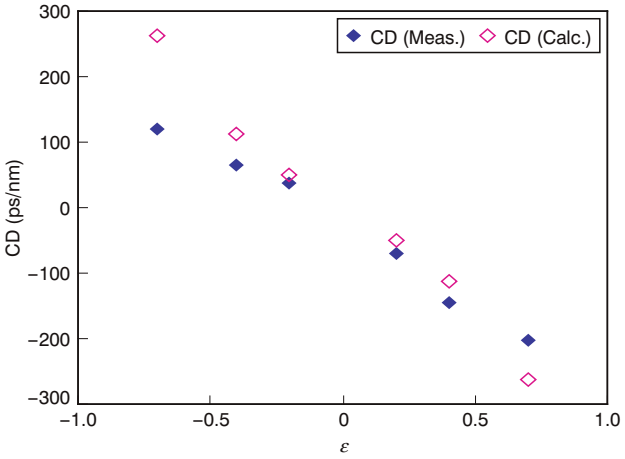


**(b) Using $G_{l2}$ target**

**Figure 10 Measured CD versus $\varepsilon$.**

From these results, we confirmed that the 8-tap transversal filter that we fabricated here works as a TDC. As has been described, this TDC can form various dispersion curve shapes using a single filter by changing tap coefficients, showing that it is suitable to compensate for the various dispersion properties in actual transmission lines.

## 7. HIGH-RESOLUTION 16-TAP TDC

As described above, even if the tap coefficient is set up precisely, an 8-tap TDC shows a narrower bandwidth and larger ripples than required in 40-Gbps systems, because the number of taps is insufficient to express sharp spectra at large $\varepsilon$ values. In order to solve this problem, we tried

fabricating a 16-tap transversal filter type TDC with high resolution to realize a large bandwidth and smaller ripples simultaneously.

Figure 11 shows the measured spectra of a 16-tap TDC at $\varepsilon = \pm 2.0$ using $G_{I1}$ target. Relative to the spectra of the 8-tap TDC in Figure 9(a), the 16-tap TDC shows a larger bandwidth, smaller ripples and the same level of CD. As a result, a CD of ±97 ps/nm, 3-dB bandwidth of about 0.5 nm, operating wavelength range of 0.6 nm and insertion loss of 17 dB were obtained.

From these results, we confirmed that increasing the number of taps is a practical method for increasing resolution, widening bandwidth and reducing ripples.

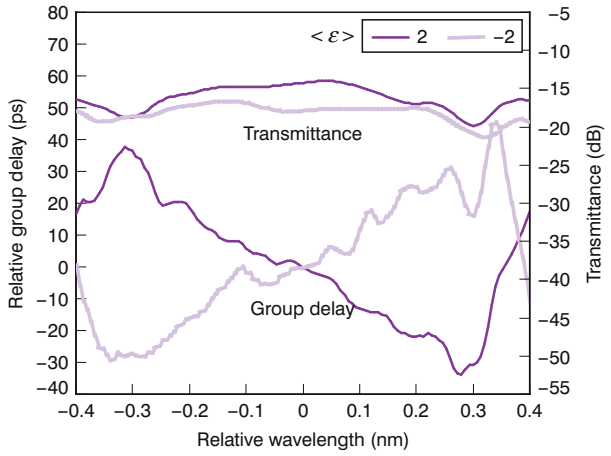


**Figure 11 Measured spectra of 16-tap TDC using $G_{I1}$ target.**

## 8. CONCLUSION

We have designed and fabricated a transversal filter type TDC in a silica-based PLC with a high index contrast of 1.5 % for dispersion compensation in high bit rate optical transmission system such as 40 Gbps.

As a result, we have been able to obtain good performance: CD of −71～+109 ps/nm, insertion loss of 10 dB, 3-dB bandwidth of 0.2 nm and operating wavelength range of 0.5 nm using a target spectrum with quadratic phase shape, and CD of −203～+121 ps/nm, insertion loss of 13 dB, 3-dB bandwidth of 0.2 nm and operating wavelength range of 0.35 nm using a target spectrum with sinusoidal phase shape.

We have also fabricated a 16-tap transversal filter type TDC with higher resolution, and have been able to obtain better performance: CD of ±97 ps/nm, insertion loss of 17 dB, 3-dB bandwidth of 0.5 nm and operating wavelength range of 0.5 nm.

For future practical use, we need to suppress ripples by improving the accuracy of tap coefficient setting, to increase resolution and pass band by increasing the number of taps, to compensate for polarization dependence, and to reduce insertion loss.

### REFERENCES

1) Y. Painchaud, M. Lapointe, and M. Guy, “Slope-Matched Tunable Dispersion Compensation over the Full C-Band Based on Fiber Bragg Gratings”, ECOC2004, We3.3.4, 2004.
2) H. Ooi, K. Nakamura, Y. Akiyama, T. Takahara, T. Terahara, Y. Kawahara, H. Isono, and G. Ishikawa, “40-Gb/s WDM Transmission With Virtually Imaged Phased Array (VIPA) Variable Dispersion Compensator”, J. Lightwave Technol., vol.20, no.12, pp.2196, 2002.
3) K. Takiguchi, K. Okamoto, and K. Moriwaki, “Planar Lightwave Circuit Dispersion Equalizer”, J. Lightwave Technol., vol.14, no.9, pp.2003, 1996.
4) K. Nara, H. Kawashima, and K. Kashihara, “Variable Dispersion Compensator using Thermo-optic Even Functional Distributed Phase Shifters formed on Arrayed-waveguides”, ECOC2003, We4. P.45, 2003.
5) N. Matsubara, H. Kawashima, and K. Nara, “Low-loss optical transversal programmable filter with symmetrical arrangement of cascade variable couplers using silica-based PLC”, proc., APOC2004, SPIE Vol. 5623-52
6) W. H. Press, et al., “Numerical Recipes in C : The Art of Scientific Computing”.
7) H. Kawashima, N. Matsubara, and K. Nara “Tunable Dispersion Compensator using Optical Transversal Filter in 1.5%-delta silica-based PLC”, proc., OECC2005, 7E3-4, 2005